Research Article

Mian Bahadur Zada, Haroon Rashid, Kamal Shah, and Thabet Abdeljawad*

Study of fractional variable order COVID-19 environmental transformation model

https://doi.org/10.1515/phys-2023-0123
received August 19, 2023; accepted October 03, 2023

Abstract: In this study, we explore the epidemic spread of the coronavirus using the Caputo fractional variable order derivative as variable order derivative provides a natural extension to classical as well as fractional order derivatives. Using the variable order derivatives in investigation of biological models of infectious diseases is an important area of research in the current time. Using the fixed point technique, we discuss the existence and uniqueness of solution to the corona virus infectious disease 2019 environmental transformation model. In order to demonstrate the existence and novelty of our findings, we examine the results numerically and graphically with the help of Euler's method. There are several graphs provided that are related to different variable orders.

Keywords: disease dynamical model, variable order differentiation, existence theory, numerical results

1 Introduction

Millions of individuals were affected by an outbreak of a serious respiratory ailment that started in December 2019 in Wuhan, China. A noval coronavirus was discovered to be the cause. After the severe acute respiratory syndrome coronavirus (SARS-CoV), which appeared in 2002 and spread to 37 countries, and the Middle East respiratory syndrome coronavirus (MERS-CoV), which appeared in 2012 and spread to 27 countries, this is the third zoonotic human coronavirus to appear in the twenty-first century. The signs and symptoms of corona virus infectious disease 2019 (COVID-19) infections frequently include a dry cough, fever, tiredness, breathing issues, and, in severe cases, bilateral lung infiltration. These symptoms are comparable to those of MERS-CoV and SARS-CoV infections [1]. Additionally, some people also had non-respiratory symptoms, such a sore throat, nausea, vomiting, and diarrhea [2,3].

Since the pandemic began, there has been a sharp rise in the number of infections caused by the coronavirus disease. On January 23, 2020, the Chinese government issued a daring order to place Wuhan and 15 other cities in Hubei under lockdown to curb the spread of the pandemic. The restriction on movement for more than 50 million people in central China is regarded as the largest quarantine in history. On January 30, 2020, the World Health Organization (WHO) formally deemed the coronavirus outbreak a Global Public Health Emergency of International Concern [4]. As of February 10, the total number of confirmed coronavirus cases in China surpassed 42,600 individuals [5]. The dynamics of COVID-19's infection are complicated by a number of elements, which makes it harder to control the disease. First, while it is commonly believed, the source of the illness is still unknown. The outbreak was started by wild creatures including bats, civets, and minks [6]. Second, according to clinical data, this condition takes between 2 and 14 days to develop. Infected persons may not have any symptoms or be unaware of their infection during this time, but they have still the capability of spreading the illness to other person [7]. Third, there are presently no antiviral medications or vaccinations available due to the recent discovery of virus. Determining and isolating symptomatic patients as soon as possible is therefore crucial for disease management. In January 2020, a significant portion of the population (hundreds of millions for the entire nation and millions for the entire city of Wuhan) traveled, which

* **Corresponding author: Thabet Abdeljawad**, Department of Mathematics and Sciences, Prince Sultan University, P.O. Box 66833, 11586 Riyadh, Saudi Arabia, e-mail: tabdeljawad@psu.edu.sa
Mian Bahadur Zada: Department of Mathematics, Government College Kabal, Swat, Khyber Pakhtunkhwa, Pakistan, e-mail: mbz.math@gmail.com
Haroon Rashid: Department of Mathematics, Government College Kabal, Swat, Khyber Pakhtunkhwa, Pakistan, e-mail: hrashid4445@gmail.com
Kamal Shah: Department of Mathematics and Sciences, Prince Sultan University, P.O. Box 66833, 11586 Riyadh, Saudi Arabia; Department of Mathematics, University of Malakand, Chakdara Dir(L), 18000, Khyber Pakhtunkhwa, Pakistan, e-mail: kamalshah408@gmail.com, kshah@psu.edu.sa

made the possibility of widespread infection transmission plausible in the past. The sickness outbreak happened just before the Spring Festival, which is China's most important festival and is commonly referred to as the Lunar New Year.

To help the health departments, and physicians, researchers of physical sciences are also trying to investigate the transmission dynamics and predict the future planning to control such diseases. In this regard, this has already been the subject of several modeling studies for the COVID-19 epidemic. The susceptible exposed infected and recovered model was created in the study by Wu *et al.* [8] to comprehend the dynamics of disease transmission. Based on data provided between December 31, 2019, and January 29, 2020, they predicted the national and worldwide spread of the disease. They also estimated that COVID-19's fundamental reproductive number was roughly 2.68 based on data fitting to an SEIR model with the supposition that the daily time steps are Poisson-distributed. Tang *et al.* [9] computed the numerical values of reproductive number. A fractional order slide mode controller was studied by Ahmed *et al.* [10]. They learn that interference strategies, such as rigorous contact tracking followed by isolation and quarantine, can successfully lower the transmission risk and the control reproduction number, which may reach 6.47. Khan *et al.* [11] used computer modeling to predict the various epidemic pathways. Additionally, Guo *et al.* [12] created a system with deep learning to assess the new coronavirus's infectiousness and forecast its prospective hosts. Their findings suggest that minks may possibly be an animal host for this virus. These models, for the most part, have demonstrated the crucial importance of the direct human-to-human transference route in this outbreak, which is further supported by the observation that the majority of people affected had no connections at all (we refer to ref. [13]). Since in the Wuhan markets, the number of cases has been rapidly increasing, and more than 20 other countries have also been affected in addition to every province in China. In particular, the COVID-19 incubation period, during which a person is exposed to the virus and when their symptoms start to manifest, ranges from 1 to 14 days. They can spread the illness to others through direct touch with ease during this time. During this time, they are symptom-free and unaware of their sickness. However, the models that have been made public so far do not take the COVID-19 gearbox's relationship to the climate into consideration. Although the majority of infected person did not wear masks and social distances. Worse still, there is a chance that the virus might remain viable in the environment for many days, raising the danger of infection through fomites and surfaces [14]. According to Geller *et al.* [15], SARS-CoV has been proven to be able to endure in such conditions. Strong evidence for the environmental survival of pathogens was found in a recent study that examined 22 different coronavirus types and discovered that coronaviruses such as SARS-CoV and MERS-CoV, and endemic human coronaviruses can survive for up to 9 days on inanimate surfaces such as metal, glass, or plastic. Additionally, a novel coronavirus that may contaminate the aquatic environment has been found in the stool of some sick persons, according to Ellerin, making fecal-oral contact a potential route of transmission for this illness [16].

A novel mathematical model for COVID-19 is proposed by Yang and Wang [17] that incorporates many transmission channels, including both the human to human and environment to human routes. In specific, they established an environmental compartment that is concerned with the concentration of pathogens in the reservoir of the environment. According to our examination, the coronavirus pandemic in humans is classified as follows: the term "susceptible" refers to the group of people who are most likely to develop the disease and are represented by X; exposure is the word used for people who are infected but do not yet show symptoms and are represented by Y; those with fully developed disease signs fall under the category of infection and are represented by I; those who have recovered from the illness are represented by M; and the viral load in the environment is denoted by the letter Q. For the transmission of the coronavirus discussed in the study by Yang and Wang [17], the classical, or integer order, model can be stated as follows:

$$\begin{cases} \dfrac{\mathrm{d}X}{\mathrm{d}t} = \Lambda - \delta X(t)Y(t) - \beta X(t)Z(t) - \nu X(t)Q(t) \\ \qquad\qquad - \sigma X(t), \\ \dfrac{\mathrm{d}Y}{\mathrm{d}t} = \delta X(t)Y(t) + \beta X(t)Z(t) - (\alpha + \sigma)Y(t), \\ \dfrac{\mathrm{d}Z}{\mathrm{d}t} = \alpha Y(t) - qZ(t), \\ \dfrac{\mathrm{d}M}{\mathrm{d}t} = \eta Z(t) - \sigma M(t), \\ \dfrac{\mathrm{d}Q}{\mathrm{d}t} = m_1 Y(t) + m_2 Z(t) - \mu Q(t), \end{cases} \tag{1}$$

and initial values as

$$X(0) = X_0 \geq 0, Y(0) = Y_0 \geq 0, Z(0) = Z_0 \geq 0, M(0) = M_0 \geq 0, Q(0) = Q_0 \geq 0.$$

Fractional derivatives are developed to describe phenomena that cannot be accurately modeled with integer-order derivatives. These phenomena often have memory or hereditary properties, meaning their current state depends on their entire past history, not just their immediate past.

This is common in physics, engineering, economics, and other fields. Fractional derivatives provide a mathematical framework for capturing these complex dynamics, making them a powerful tool for analysis and modeling. There exists a wide area of literature that explores the different forms of fractional derivatives and their applications [18,19]. It is crucial to observe that each of the fractional derivative order definition has its benefits as well as drawbacks. Using fractional order derivatives many authors have studied various models like we refer to previous studies [20–23].

A variable order fractional derivative and integral first proposed by Samko and Ross [24] extended the constant order RL-integration to variable order. The variable order integral was then used to define the variable order RL-differential operator. This type of derivative is useful in modeling complex systems that exhibit behaviors that change over time or space. The fractional variable order derivative is a powerful tool for modeling complex systems that exhibit non-local and non-linear behavior. Its applications are vast and diverse, and it has the potential to revolutionize the way we understand and model complex systems in various fields. Coimbra [25] proposed the variable order Caputo differential operator to address some of the limitations of the variable order RL-fractional derivative. While the Caputo-fractional derivative is a valuable tool, it does have some limitations. The Caputo–Fabrizio (CF) variable order fractional derivative [26,27] was introduced to address some of the limitations of the Caputo-fractional derivative in certain situations. This derivative has the standard properties of classical derivatives. The CF-fractional derivative is a non-local operator that is defined in terms of an exponential decay kernel. Unlike the classical CF-fractional derivative, it does not involve singularities at the initial time. This makes it more suitable for describing physical phenomena where the memory fades away exponentially. Since variable order operators are the natural extension of classical ordinary as well as fractional orders such operators are used as a sophisticated tool to study the dynamical systems of infectious disease. Recently, Bushnaq *et al.* [28] studied a two-compartment *SI* model of COVID-19 using variable order derivative. For more significant contribution using variable orders derivatives, we refer to previous studies [29–31].

Motivated from the aforementioned importance and applications of variable order differentiations and integrations, we consider Model 1 under the variable order and subject to the same initial data as:

$$\begin{cases} {}^{c}D_{t}^{\theta(x)}X(t) = \Lambda - \delta X(t)Y(t) - \beta X(t)Z(t) - \nu X(t)Q(t), \\ {}^{c}D_{t}^{\theta(x)}Y(t) = \delta X(t)Y(t) + \beta X(t)Z(t) - (\alpha + \sigma)Y(t), \\ {}^{c}D_{t}^{\theta(x)}Z(t) = \alpha Y(t) - qZ(t), \\ {}^{c}D_{t}^{\theta(x)}M(t) = \eta Z(t) - \sigma M(t), \\ {}^{c}D_{t}^{\theta(x)}Q(t) = m_1 Y(t) + m_2 Z(t) - \mu Q(t), \end{cases} \tag{2}$$

where $\theta : [0, T] \to (0, 1]$ is the continuous function in $x \in [0, T]$. We first establish the existence theory for the considered model using the Banach and Schaefer fixed point theorems (for details, we refer to Schaefer [32]). Furthermore, for numerical interpretation, we use Euler's method. The corresponding results are presented graphically using MatLab. In addition, we state that relevant applications of variable order problems and their numerical analysis have been done in the last few years very well. In this regard, we refer to some significant work as previous studies [33–37]. Following the mentioned work, we also attempt on the numerical investigation of our considered model using Euler's method and present the obtained results graphically for various variable orders.

2 Preliminaries

In this section, we recall some basic facts, results, and definitions.

Theorem 2.1. [32] *Let $\Lambda \subset \Xi$ be a nonempty convex, closed and bounded set, then a complete continuous operator $\Upsilon : \Lambda \to \Lambda$ with $\Upsilon(\Lambda) \subset \Xi$ has a fixed point in Λ.*

Definition 2.2. [24] Let $\theta : [0, T] \to (0, 1]$ be continuous function, then variable order integration for $f \in L[0, T]$ is defined as:

$$I_t^{\theta(x)} f(t) = \frac{1}{\Gamma(\theta(x))} \int_0^t (t - \varrho)^{\theta(x)-1} f(\varrho) d\varrho, \quad \forall x, t \in [0, T],$$

such that the right-hand side converges pointwise.

Definition 2.3. [33] For the continuous function $\theta : [0, T] \to (0, 1]$, variable order derivative for $f \in C[0, T]$ is defined by:

$$\mathrm{D}_t^{\theta(x)} f(t) = \frac{1}{\Gamma(1 - \theta(x))} \int_0^t (t - \varrho)^{-\theta(x)} f'(\varrho) d\varrho, \quad \forall x, t \in [0, T],$$

provided that the integral on right-hand side converges.

Lemma 2.3.1. [34] *If* $\theta : [0, T] \to (0, 1]$, $h \in L[0, T]$, *and* $f \in C[0, T] \cup L(0, T)$, *then the solution of variable order problem*

$$D_t^{\theta(x)} f(t) = h(t), \quad x, t \in [0, T],$$

is described as:

$$f(t) = a_0 + \frac{1}{\Gamma(\theta(x))} \int_0^t (t - \varrho)^{\theta(x)-1} f(\varrho) d\varrho, \quad x, t \in [0, T].$$

3 Qualitative analysis

The qualitative theory of the existence of a solution to a dynamical system, which enables us to determine whether a problem has a solution or not, is a significant outcome of the applied analysis. A crucial technique for determining the existence and uniqueness of the solution to a dynamical system in this context is fixed point theory. First, we create the model (2) as:

$$\begin{cases} {}^cD_t^{\theta(x)} X(t) = \mathfrak{F}_1(X, Y, Z, M, Q), \\ {}^cD_t^{\theta(x)} Y(t) = \mathfrak{F}_2(X, Y, Z, M, Q), \\ {}^cD_t^{\theta(x)} Z(t) = \mathfrak{F}_3(X, Y, Z, M, Q), \\ {}^cD_t^{\theta(x)} M(t) = \mathfrak{F}_4(X, Y, Z, M, Q), \\ {}^cD_t^{\theta(x)} Q(t) = \mathfrak{F}_5(X, Y, Z, M, Q), \end{cases} \tag{3}$$

where $\mathfrak{F}_1(X, Y, Z, M, Q) = \lambda - \delta XY - \beta XZ - \nu XQ - \sigma X$, $\mathfrak{F}_2(X, Y, Z, M, Q) = \delta XY + \beta XZ - (\alpha + \sigma)Y$, $\mathfrak{F}_3(X, Y, Z, M, Q) = \alpha Y - qZ$,$\mathfrak{F}_4(X, Y, Z, M, Q) = \eta Z - \sigma M$, and $\mathfrak{F}_5(X, Y, Z, M, Q) = m_1 Y + m_2 Z - \mu Q$. Now, applying variable order integral $I_t^{\theta(x)}$ to both sides of the model (3), we obtain

$$\begin{cases} X(t) = X_0 + \frac{1}{\Gamma(\theta(x))} \int_0^t (t - \varrho)^{\theta(x)-1} [\mathfrak{F}_1(X, Y, Z, M, Q)] d\varrho, \\ Y(t) = Y_0 + \frac{1}{\Gamma(\theta(x))} \int_0^t (t - \varrho)^{\theta(x)-1} [\mathfrak{F}_2(X, Y, Z, M, Q)] d\varrho, \\ Z(t) = Z_0 + \frac{1}{\Gamma(\theta(x))} \int_0^t (t - \varrho)^{\theta(x)-1} [\mathfrak{F}_3(X, Y, Z, M, Q)] d\varrho, \\ M(t) = M_0 + \frac{1}{\Gamma(\theta(x))} \int_0^t (t - \varrho)^{\theta(x)-1} [\mathfrak{F}_4(X, Y, Z, M, Q)] d\varrho, \\ Q(t) = Q_0 + \frac{1}{\Gamma(\theta(x))} \int_0^t (t - \varrho)^{\theta(x)-1} [\mathfrak{F}_5(X, Y, Z, M, Q)] d\varrho. \end{cases}$$

The aforementioned system can be represented as:

$$\mathfrak{B}(t) = \mathfrak{B}_0 + \frac{1}{\Gamma(\theta(x))} \int_0^t (t - \varrho)^{\theta(x)-1} \mathfrak{D}(\varrho, \mathfrak{B}(\varrho)) d\varrho, \tag{4}$$

where $\mathfrak{B}(t)$ is one of $X(t), Y(t), Z(t), M(t)$, and $Q(t)$, $\mathfrak{B}_0$ is one of X_0, Y_0, Z_0, M_0, and Q_0, and $\mathfrak{D}(t, \mathfrak{B}(t))$ is one of $\mathfrak{F}_1(X, Y, Z, M, Q)$, $\mathfrak{F}_2(X, Y, Z, M, Q)$, $\mathfrak{F}_3(X, Y, Z, M, Q)$,

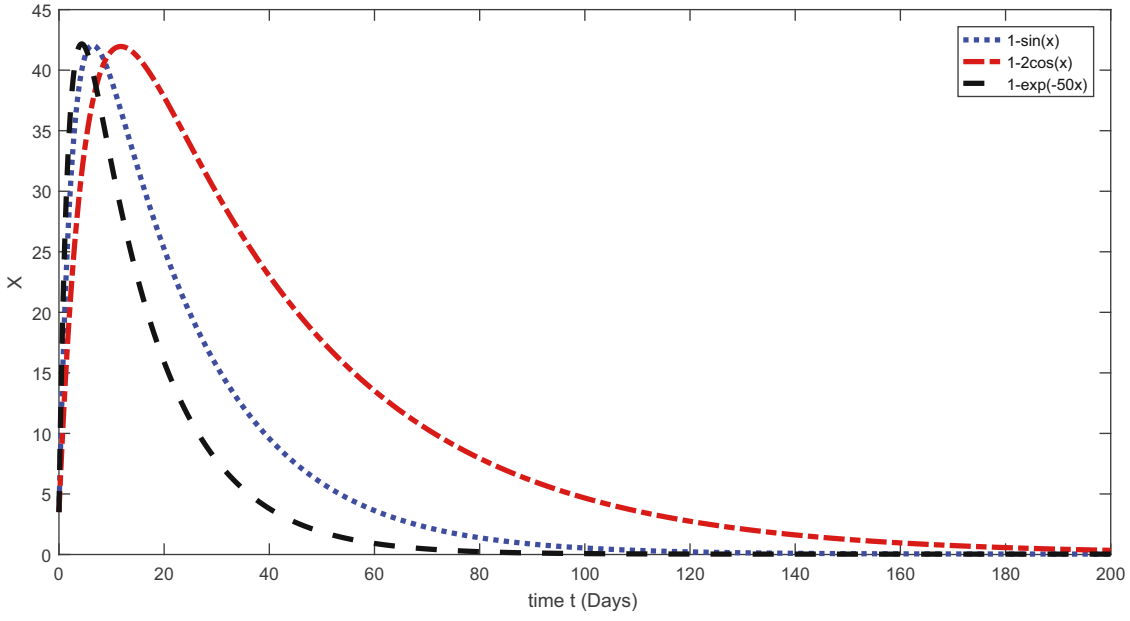

Figure 1: Graphical representation of the estimated X solution using several variable orders.

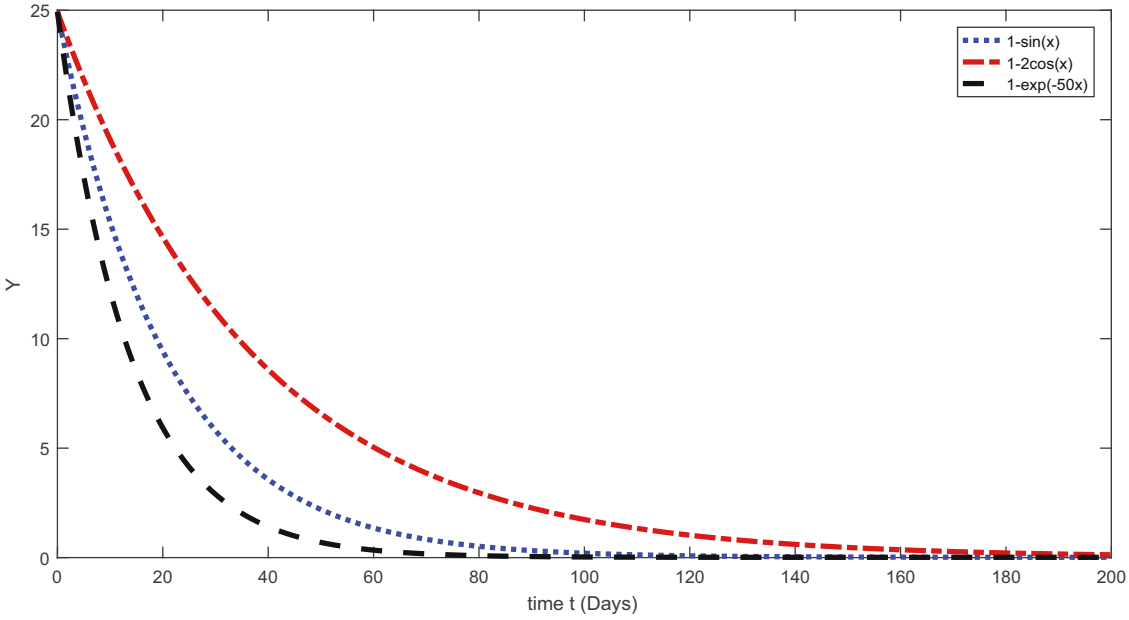

Figure 2: Graphical representation of the estimated Y solution using several variable orders.

$\mathfrak{F}_4(X, Y, Z, M, Q)$, and $\mathfrak{F}_5(X, Y, Z, M, Q)$. Furthermore, we suppose a bounded and closed set $[0, T]$. Additionally, let $\mathfrak{D} = C([0, T] \times R^5, R)$ be a Banach space with the norm $\|\xi\| = \max_{t\in[0,T]}\{|\xi(t)| : \xi = (X, Y, Z, M, Q), T > 0\}$. Now, to establish the existence results for the model (2), we assume the following assertions:

(A1) For every $\mathfrak{B}, \bar{\mathfrak{B}} \in \mathfrak{D}$, there exists constant $\mathfrak{C}_{\mathfrak{D}} > 0$ such that

$$|\mathfrak{D}(t, \mathfrak{B}(t)) - \mathfrak{D}(t, \bar{\mathfrak{B}}(t))| \leq \mathfrak{C}_{\mathfrak{D}}\|\mathfrak{B} - \bar{\mathfrak{B}}\|.$$

(A2) For every $\mathfrak{B} \in \mathfrak{D}$, there exists constant $\mathfrak{H}_{\mathfrak{D}}, \mathfrak{Z}_{\mathfrak{D}} > 0$ such that

$$|\mathfrak{D}(t, \mathfrak{B}(t))| \leq \mathfrak{H}_{\mathfrak{D}}\|\mathfrak{B}\| + \mathfrak{Z}_{\mathfrak{D}}.$$

Theorem 3.1. *In view of hypothesis* (A_2), *Model* (2) *has at least one solution.*

Proof. Assume that $\mathbf{B} = \{\mathfrak{B} \in \mathfrak{D} : \|\mathfrak{B}\| \leq r\}$, with $r \geq \frac{|\mathfrak{B}_0| \Gamma(\theta(x)+1) + T^{\theta(x)}[\mathfrak{H}_{\mathfrak{D}} r + \mathfrak{Z}_{\mathfrak{D}}]}{\Gamma(\theta(x)+1)}$. Define the operator $\mathfrak{A} : \mathbf{B} \to \mathbf{B}$ as:

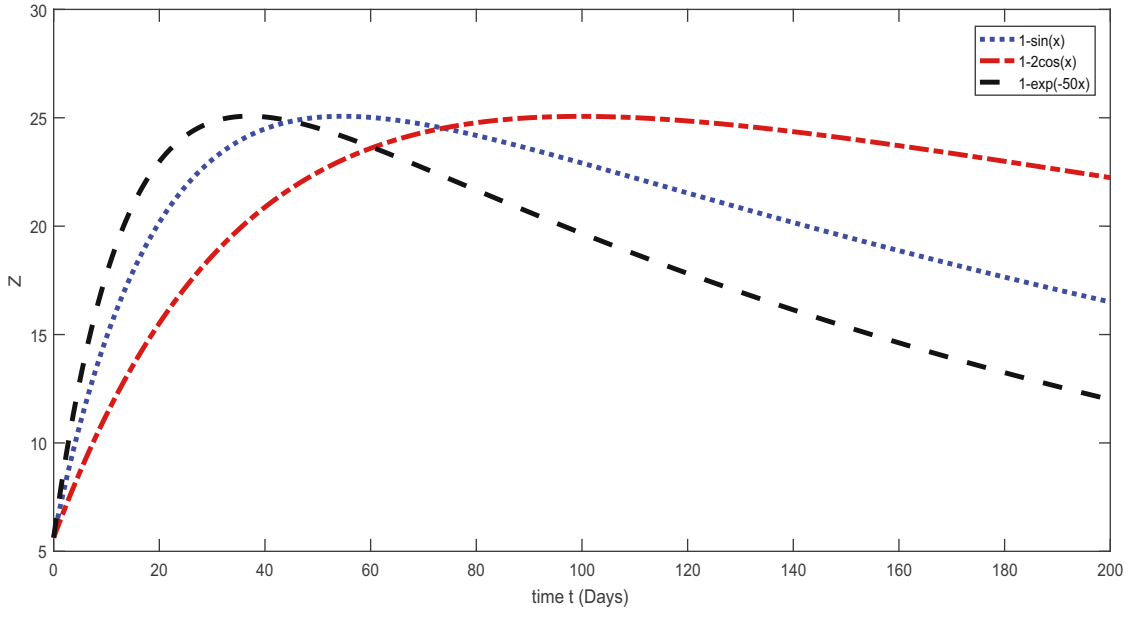

Figure 3: Graphical representation of the estimated Z solution using several variable orders.

$$\mathfrak{A}(\mathfrak{B}) = \mathfrak{B}_0 + \frac{1}{\Gamma(\theta(x))}\int_0^t (t-\varrho)^{\theta(x)-1}\mathfrak{D}(\varrho, \mathfrak{B}(\varrho))d\varrho. \quad (5)$$

Then, for every $\mathfrak{B} \in \mathbf{B}$, we have

$$\begin{aligned}
|\mathfrak{A}(\mathfrak{B})| &\le |\mathfrak{B}_0| + \frac{1}{\Gamma(\theta(x))}\int_0^t (t-\varrho)^{\theta(x)-1}|\mathfrak{D}(\varrho, \mathfrak{B}(\varrho))|d\varrho \\
&\le |\mathfrak{B}_0| + \frac{1}{\Gamma(\theta(x))}\int_0^t (t-\varrho)^{\theta(x)-1}[\mathfrak{H}_{\mathfrak{D}}|\mathfrak{B}| + \mathfrak{Z}_{\mathfrak{D}}]d\varrho \\
&= |\mathfrak{B}_0| + \frac{T^{\theta(x)}}{\Gamma(\theta(x)+1)}[\mathfrak{H}_{\mathfrak{D}}\|\mathfrak{B}\| + \mathfrak{Z}_{\mathfrak{D}}] \\
&\le |\mathfrak{B}_0| + \frac{T^{\theta(x)}}{\Gamma(\theta(x)+1)}[\mathfrak{H}_{\mathfrak{D}} r + \mathfrak{Z}_{\mathfrak{D}}] \\
&\le r,
\end{aligned}$$

i.e., $\|\mathfrak{A}(\mathfrak{B})\| \le r$, and hence, $\mathfrak{A}(\mathfrak{B}) \in \mathbf{B}$. Therefore one has $\mathfrak{A}(\mathbf{B}) \subset \mathbf{B}$. Also, it is obvious that $\mathbf{B}$ is bounded. Assume that $t_m, t_n \in [0, T]$, such that $t_m < t_n \in [0, T]$, then consider

$$\begin{aligned}
&|\mathfrak{A}(\mathfrak{B})(t_n) - \mathfrak{A}(\mathfrak{B})(t_m)| \\
&= \left| \frac{1}{\Gamma(\theta(x))}\int_0^t (t_n-\varrho)^{\theta(x)-1}\mathfrak{D}(\varrho, \mathfrak{B}(\varrho))d\varrho \right. \\
&\quad \left. - \frac{1}{\Gamma(\theta(x))}\int_0^t (t_m-\varrho)^{\theta(x)-1}\mathfrak{D}(\varrho, \mathfrak{B}(\varrho))d\varrho \right| \\
&\le \left[\frac{1}{\Gamma(\theta(x))}\int_0^t [(t_m-\varrho)^{\theta(x)-1} - (t_n-\varrho)^{\theta(x)-1}]|\mathfrak{D}(\varrho, \mathfrak{B}(\varrho))|d\varrho \right. \\
&\quad \left. + \int_{t_m}^{t_n} (t_n-\varrho)^{\theta(x)-1}|\mathfrak{D}(\varrho, \mathfrak{B}(\varrho))|d\varrho \right] \\
&\le \frac{(\mathfrak{H}_{\mathfrak{D}} r + \mathfrak{Z}_{\mathfrak{D}})}{\Gamma(\theta(x)+1)}[t_m^{\theta(x)} - t_n^{\theta(x)} + 2(t_n - t_m)^{\theta(x)}].
\end{aligned}$$

As $t_m \to t_n$, then right-hand side goes to zero in the aforementioned equation. Also, $\mathfrak{A}$ is bounded and continuous. Therefore,

$$\|\mathfrak{A}(\mathfrak{B})(t_n) - \mathfrak{A}(\mathfrak{B})(t_m)\| \to 0, \quad \text{as } t_m \to t_n.$$

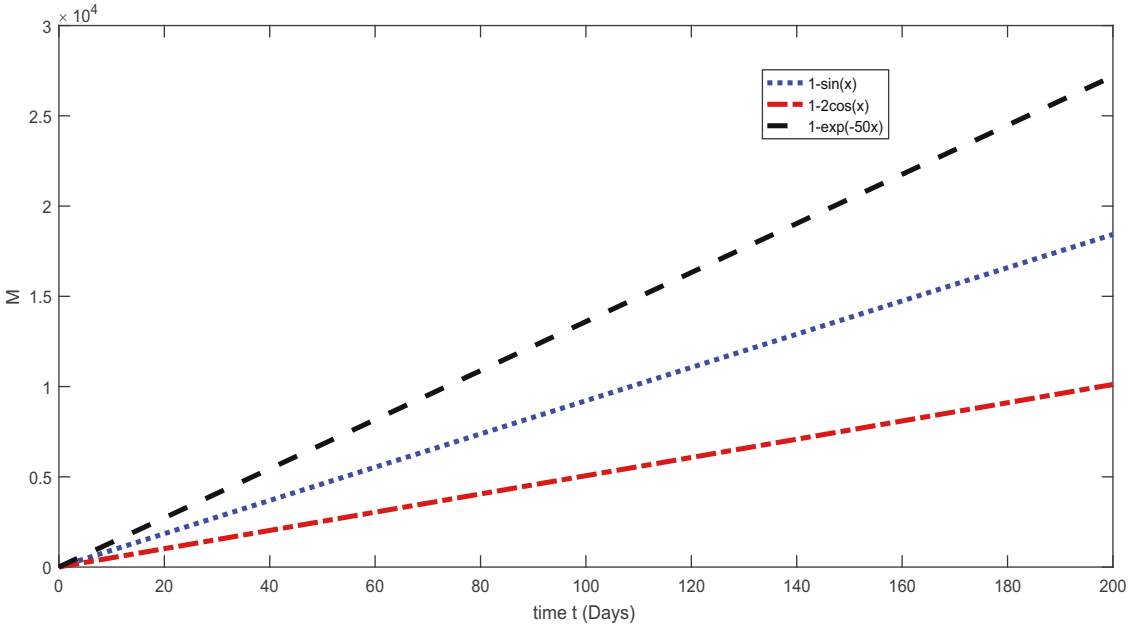

Figure 4: Graphical representation of the estimated M solution using several variable orders.

Thus, $\mathfrak{A}$ is completely continuous function. Therefore, by Theorem 2.1, $\mathfrak{A}$ has a fixed point. Consequently, Model (2) has at least one solution. □

Theorem 3.2. *In view of hypothesis* (A_1), *Model* (2) *has a unique solution if* $\frac{\mathfrak{C}_{\mathfrak{D}}T^{\theta(x)}}{\Gamma(\theta(x)+1)} < 1$.

Proof. We define the operator $\mathfrak{F} : \mathfrak{D} \to \mathfrak{D}$ as:

$$\mathfrak{F}(\mathfrak{B}) = \mathfrak{B}_0 + \frac{1}{\Gamma(\theta(x))}\int_0^t (t-\varrho)^{\theta(x)-1}\mathfrak{D}(\varrho, \mathfrak{B}(\varrho))d\varrho.$$

Proceeding, we take $\mathfrak{B}, \bar{\mathfrak{B}} \in \mathfrak{D}$, and consider

$$\begin{aligned}\|\mathfrak{F}(\mathfrak{B}) - \mathfrak{F}(\bar{\mathfrak{B}})\| &= \max_{t\in[0,T]} \left| \frac{1}{\Gamma(\theta(x))}\int_0^t (t-\varrho)^{\theta(x)-1}\mathfrak{D}(\varrho, \mathfrak{B}(\varrho))d\varrho \right.\\ &\quad \left. - \frac{1}{\Gamma(\theta(x))}\int_0^t (t-\varrho)^{\theta(x)-1}\mathfrak{D}(\varrho, \bar{\mathfrak{B}}(\varrho))d\varrho \right|\\ &\le \max_{t\in[0,T]} \frac{1}{\Gamma(\theta(x))}\int_0^t (t-\varrho)^{\theta(x)-1}|\mathfrak{D}(\varrho, \mathfrak{B}(\varrho))\\ &\quad - \mathfrak{D}(\varrho, \bar{\mathfrak{B}}(\varrho))|d\varrho\\ &\le \frac{\mathfrak{C}_{\mathfrak{D}}T^{\theta(x)}}{\Gamma(\theta(x)+1)}\|\mathfrak{B} - \bar{\mathfrak{B}}\|.\end{aligned}$$

Since $\frac{\mathfrak{C}_{\mathfrak{D}}T^{\theta(x)}}{\Gamma(\theta(x)+1)} < 1$, which yields that $\mathfrak{F}$ is a contraction. As a conclusion by the Banach contraction principle, the proposed model (2) has a unique solution. □

4 Interpretation *via* numerical scheme

The numerical outcomes of a variable order system can be computed using a variety of numerical approaches. Here, we analyze Model (2) solution using the fractional Euler's approach [28]. The formula for Euler's approach to the Caputo fractional variable order derivative is as follows:

$$t_{j+1} = t_j + h, \tag{6}$$

$$f(t_{j+1}) = f(t_j) + \frac{h^{\theta(x)}}{\Gamma(a+1)}G(t_j, f(t_j)), \quad j = 0, 1, \ldots, n-1, \tag{7}$$

where h is a step size. It can be easily observed that for $\theta(x) = 1$, the aforementioned approach becomes the standard Euler approach. Now, using the beginning

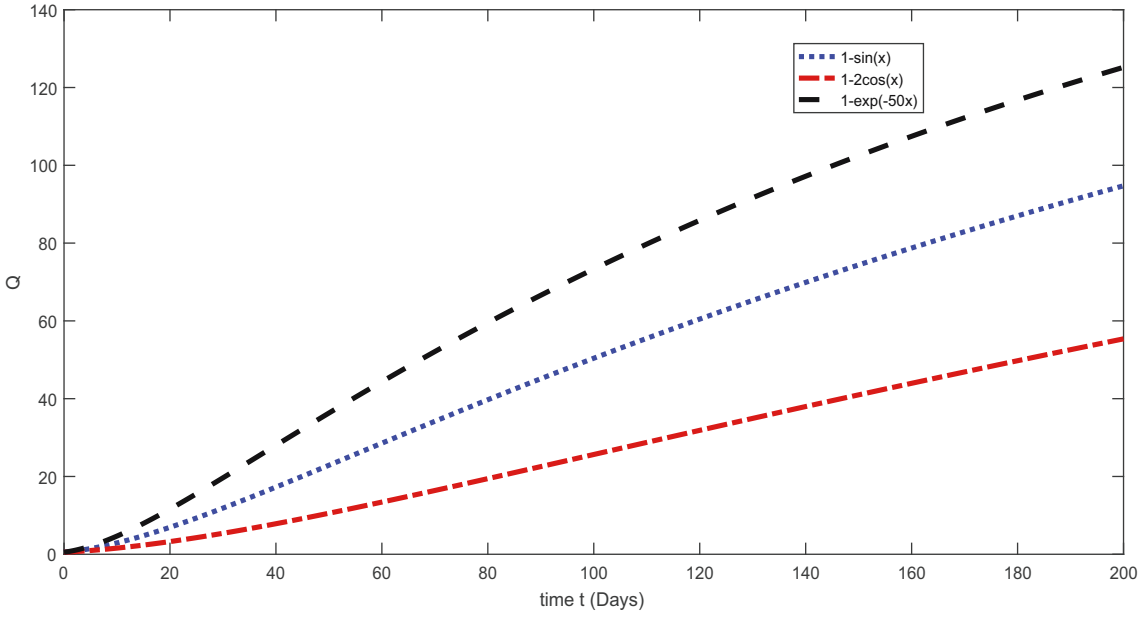

Figure 5: Graphical representation of the estimated Q solution using several variable orders.

circumstances and parameter values, we numerically solve the fractional Model (2). Using the values as $\Lambda = 271.23$, $\delta = 3.11 \times 10^{-8}$, $\beta = 0.62 \times 10^{-8}$, $\nu = 1.03 \times 10^{-8}$, $\sigma = 3.01 \times 10^{-5}$, $\alpha = \frac{1}{7}$, $q = 0.01$, $\eta = \frac{1}{15}$, $m_1 = 2.30$, $m_1 = 2.30$, $m_2 = 0$, $\mu = 1$, $X_0 = 7.50$ mm, $Y_0 = 24.39$ mm, $Z_0 = 5.63$ mm, $M_0 = 0.52$ mm, and $Q_0 = 3.50$ mm, now, the fractional Model (2) with the iterative Formula (7) becomes

$$\begin{aligned}
X(t_{i+1}) &= X_0 + \frac{h^{\theta(x)}}{\Gamma(\theta(x)+1)}(271.23 - 3.11 \times 10^{-8}X(t_i)Y(t_i) \\
&\quad - 0.62 \times 10^{-8}X(t_i)Z(t_i) - 1.03 \times 10^{-8}X(t_i)Q(t_i) \\
&\quad - 3.01 \times 10^{-5}X(t_i)), \\
Y(t_{i+1}) &= Y_0 + \frac{h^{\theta(x)}}{\Gamma(\theta(x)+1)}\Big(3.11 \times 10^{-8}X(t_i)Y(t_i) \\
&\quad + 0.62 \times 10^{-8}X(t_i)Z(t_i) - \Big(\frac{1}{7} + 3.01 \times 10^{-5}\Big)Y(t_i)\Big), \\
Z(t_{i+1}) &= Z_0 + \frac{h^{\theta(x)}}{\Gamma(\theta(x)+1)}\Big(\frac{1}{7}Y(t_i) - 0.01Z(t_i)\Big), \\
M(t_{i+1}) &= M_0 + \frac{h^{\theta(x)}}{\Gamma(\theta(x)+1)}\Big(\frac{1}{15}Z(t_i) - 3.01 \times 10^{-5}M(t_i)\Big), \\
Q(t_{i+1}) &= Q_0 + \frac{h^{\theta(x)}}{\Gamma(\theta(x)+1)}(2.30Y(t_i) + 0Z(t_i) - Q(t_i)),
\end{aligned}$$

where $x \in [0, T]$. By solving the aforementioned iterative system, the numerical solution for different values of $\theta(x)$ is obtained using MatLab.

Using different choices of fractional order, we have graphically illustrated the approximate solutions for the various compartments of the proposed model $\theta(x)$ in Figures 1–5. The decay in susceptible population with variable orders is shown in Figure 1. In the same way, we observe decline in the density of class Y (see Figure 2). Moreover, the increase or growth has been appeared in other three compartments in Figures 3–5, respectively. From these interpretations, we conclude that variable orders are more legalistic approach to investigate dynamical systems numerically.

5 Conclusion

For a dynamical model of COVID-19, we have constructed a qualitative examination of the existence and uniqueness of solution. In addition to understand the transmission dynamics of the proposed model, we have used Euler's numerical method. Variable order differentiation, equivalent to a continuous function, has been used as $\theta : [0, T] \to (0, 1]$. We have used the fixed point theory for the qualitative results. Because using the fixed point theory, we can investigate the existence of solution to the considered problem. In addition, Euler's method was extended to establish a numerical scheme for graphical presentation to various classes of the considered model. We have presented the numerical solution graphically by considering three variable order values such as $\theta(x) = 1 - \sin(x), 1 - 2\cos(x)$, and $1 - \exp(-50x)$, $x \in [0, T]$ in Figures 1–5, respectively. From graphical presentation, the concerned dynamical behavior of decay in susceptible exposed classes, while growth in the compartments Z, M, and Q can be clearly observable. In the future, we will extend our aforesaid analysis to variable order fractals-fractional model for more sophisticated analysis and the complex geometry involved behind it.

Acknowledgments: The authors appreciate the Prince Sultan University for APC and support through TAS research lab.

Funding information: The Prince Sultan University for APC and support through TAS research lab.

Author contributions: All authors have accepted responsibility for the entire content of this manuscript and approved its submission.

Conflict of interest: The authors state no conflict of interest.

References

[1] Gralinski LE, Menachery VD. Return of the Coronavirus: 2019-nCoV. Viruses. 2020;12(2):135.

[2] Maxmen A, Mallapaty S. The COVID lab-leak hypothesis: what scientists do and donat know. Nature. 2021;594(7863):313–5.

[3] Garcia M, Lipskiy N, Tyson J, Watkins R, Esser ES, Kinley T. Centers for Disease Control and Prevention 2019 novel coronavirus disease (COVID-19) information management: addressing national healthcare and public health needs for standardized data definitions and codified vocabulary for data exchange. J Amer Med Infor Assoc. 2020;27(9):1476–87.

[4] World Health Organization, WHO statement regarding the outbreak of novel coronavirus (2019-nCoV), 2020.

[5] Chiodini J. Maps, masks and media-Traveller and practitioner resources for 2019 novel coronavirus (2019-nCoV) acute respiratory virus. Travel Med Infect Disease. 2020;33:101574.

[6] Zhou P, Yang XL, Wang XG, Hu B, Zhang L, Zhang W, et al. Discovery of a novel coronavirus associated with the recent pneumonia outbreak in humans and its potential bat origin. BioRxiv. 2020:2020–01. https://doi.org/10.1101/2020.01.22.914952.

[7] Rothe C, Schunk M, Sothmann P, Bretzel G, Froeschl G, Wallrauch C, et al. Transmission of 2019-nCoV infection from an asymptomatic contact in Germany. N Eng J Med. 2020;382(10):970–1.

[8] Wu JT, Leung K, Leung GM. Nowcasting and forecasting the potential domestic and international spread of the 2019-nCoV outbreak originating in Wuhan, China: a modelling study. The Lancet. 2020;395(10225):689–97.
[9] Tang B, Bragazzi NL, Li Q, Tang S, Xiao Y, Wu J. An updated estimation of the risk of transmission of the novel coronavirus (2019-nCov). Infect Disease Model. 2020;5:248–55.
[10] Ahmed S, Azar AT, Tounsi M. Design of adaptive fractional-order fixed-time sliding mode control for robotic manipulators. Entropy. 2022;24(12):1838.
[11] Khan H, Li Y, Khan A, Khan A. Existence of solution for a fractional-order Lotka-Volterra reaction-diffusion model with Mittag-Leffler kernel. Math Meth Appl Sci. 2019;42(9):3377–87.
[12] Guo Q, Li M, Wang C, Wang P, Fang Z, Tan J, et al. Host and infectivity prediction of Wuhan 2019 novel coronavirus using deep learning algorithm. BioRxiv. 2020:2020–01.
[13] Chan JF, Yuan S, Kok KH, To KK, Chu H, Yang J, et al. A familial cluster of pneumonia associated with the 2019 novel coronavirus indicating person-to-person transmission: a study of a family cluster. The Lancet. 2020;395(10223):514–23.
[14] Cheng ZJ, Shan J. 2019 Novel Coronavirus: where we are and what we know. Infection. 2020;48:155–63.
[15] Geller C, Varbanov M, Duval RE. Human coronaviruses: insights into environmental resistance and its influence on the development of new antiseptic strategies. Viruses. 2012;4(11):3044–68.
[16] Kampf G, Todt D, Pfaender S, Steinmann E. Persistence of coronaviruses on inanimate surfaces and their inactivation with biocidal agents. J Hospital Infect. 2020;104(3):246–51.
[17] Yang C, Wang J. A mathematical model for the novel coronavirus epidemic in Wuhan, China. Math Biosci Eng MBE. 2020;17(3):2708.
[18] Caputo M. Linear models of dissipation whose Q is almost frequency independent-II. Geophy J Int. 1967;13(5):529–39.
[19] Caputo M, Fabrizio M. A new definition of fractional derivative without singular kernel. Prog Frac Diff Appl. 2015;1(2):73–85.
[20] Bushnaq S, Saeed T, Torres DF, Zeb A. Control of COVID-19 dynamics through a fractional-order model. Alexandr Eng J. 2021;60(4):3587–92.
[21] Khan H, Alzabut J, Baleanu D, Alobaidi G, Rehman MU. Existence of solutions and a numerical scheme for a generalized hybrid class of n-coupled modified ABC-fractional differential equations with an application. AIMS Math. 2023;8(3):6609–25.
[22] Maayah B, Moussaoui A, Bushnaq S, Abu Arqub O. The multistep Laplace optimized decomposition method for solving fractional-order coronavirus disease model (COVID-19) via the Caputo fractional approach. Demonstr Math. 2022;55(1):963–77.
[23] Razminia A, Dizaji AF, Majd VJ. Solution existence for non-autonomous variable-order fractional differential equations. Math Comput Model. 2012;55(3–4):1106–17.
[24] Samko SG, Ross B. Integration and differentiation to a variable fractional order. Integral Transform Spec Funct. 1993;1(4):277–300.
[25] Coimbra CF. Mechanics with variablee-order differential operators. Ann Phys. 2003;515(11–12):692–703.
[26] Alharthi NH, Jeelani MB. A fractional model of COVID-19 in the frame of environmental transformation with Caputo fractional derivative. Adv Appl Stat. 2023;88(2):225–44.
[27] Zheng X, Wang H, Fu H. Well-posedness of fractional differential equations with variable-order Caputo–Fabrizio derivative. Chaos Solitons Fractals. 2020;138:109966.
[28] Bushnaq S, Sarwar M, Alrabaiah H. Existence theory and numerical simulations of variable order model of infectious disease. Results Appl Math. 2023;19:100395.
[29] Heydari MH, Atangana A. A cardinal approach for nonlinear variable-order time fractional Schrödinger equation defined by Atangana-Baleanu-Caputo derivative. Chaos Solitons Fractals. 2019;128:339–48.
[30] Atangana A, Botha JF. A generalized groundwater flow equation using the concept of variable-order derivative. Boundary Value Problems. 2013;2013:1.
[31] Atangana A. Fractional operators with constant and variable order with application to geo-hydrology. New York: Academic Press; 2017 Sep 19.
[32] Schaefer H. Über die Methode der a priori-Schranken. Mathematische Annalen. 1955;129(1):415–6.
[33] Soon CM, Coimbra CF, Kobayashi MH. The variable viscoelasticity oscillator. Annalen der Physik. 2005;517(6):378–89.
[34] Lin R, Liu F, Anh V, Turner I. Stability and convergence of a new explicit finite-difference approximation for the variable-order nonlinear fractional diffusion equation. Appl Math Comput. 2009;212(2):435–45.
[35] Arafa AA, Khalil M, Sayed A. A non-integer variable order mathematical model of human immunodeficiency virus and malaria coinfection with time delay. Complexity. 2019;2019:4291017.
[36] Gómez-Aguilar JF. Analytical and numerical solutions of a nonlinear alcoholism model via variable-order fractional differential equations. Phys A Stat Mech Appl. 2018;494:52–75.
[37] Hammouch Z, Yavuz M, Özdemir N. Numerical solutions and synchronization of a variable-order fractional chaotic system. Math Model Numer Simulat Appl. 2021;1(1):11–23.